LAWRENCE
LIVERMORE
NATIONAL
LABORATORY

LLNL-JRNL-400067

MICROPATTERNING OF GOLD SUBSTRATES BASED ON POLY(PROPYLENE SULFIDE-BL-ETHYLENE GLYCOL), (PPS-PEG) BACKGROUND PASSIVATION AND THE MOLECULAR-ASSEMBLY PATTERNING BY LIFT-OFF (MAPL) TECHNIQUE

L. Feller, J. P. Bearinger, L. Wu, J. A. Hubbell, M. Textor, S. Tosatti

December 21, 2007

Surface Science

Disclaimer

MICROPATTERNING OF GOLD SUBSTRATES BASED ON POLY(PROPYLENE SULFIDE-*BL*-ETHYLENE GLYCOL), (PPS-PEG) BACKGROUND PASSIVATION AND THE MOLECULAR-ASSEMBLY PATTERNING BY LIFT-OFF (MAPL) TECHNIQUE

L. Feller[1], J.P. Bearinger[2], L. Wu[2], J. A. Hubbell[3], M. Textor[1], S. Tosatti[1]

Corresponding Author: J.P. Bearinger

[1.] BioInterface Group, Laboratory for Surface Science and Technology, Swiss Federal Institute of Technology (ETH), Zurich, Switzerland

[2]. Applied Physics and Biophysics, Lawrence Livermore National Laboratory, Livermore, CA, 94550, USA

[3.] Integrative Biosciences Institute and Institute for Chemical Science and Engineering, Ecole Polytechnique Fédérale de Lausanne, Lausanne, Switzerland

Abstract

Poly(propylene sulfide-*bl*-ethylene glycol (PPS-PEG) is an amphiphilic block copolymer that spontaneously adsorbs onto gold from solution. This results in the formation of a stable polymeric layer that renders the surface protein resistant when an appropriate architecture is chosen. The established molecular assembly patterning by lift-off (MAPL) technique can convert a prestructured resist film into a pattern of

biointeractive chemistry and a noninteractive background. Employing the MAPL technique, we produced a micron-scale PPS-PEG pattern on a gold substrate, and then characterized the patterned structure with Time-of-Flight Secondary Ion Mass Spectrometry (TOF-SIMS) and Atomic Force Microscopy (AFM). Subsequent exposure of the PPS-PEG /gold pattern to protein adsorption (full human serum) was monitored *in situ*; SPR-imaging shows a selective adsorption of proteins on gold, but not on PPS-PEG areas. Analysis shows a reduction of serum adsorption up to 93% on the PPS-PEG areas as compared to gold, in good agreement with previous analysis on homogenously adsorbed PPS-PEG on gold. MAPL patterning of PPS-PEG block copolymers fast, versatile and reproducible, and allows for subsequent use of biosensor-based surface analysis methods.

Keywords

biosensing, photolithography, Tof-SIMS, Surface Plasmon techniques, adsorption, patterning, self-assembly, gold

1. Introduction

The lab-on-a-chip modality of a single sensor comprised of numerous chemical functionalities allows for simultaneous immobilization and/or analysis of complex molecules [1-3]. Design and quality of the chip surface are essential for performance. High signal-to-noise ratios require 1) a non-interactive background and 2) high affinity towards captured molecules. Quantification of the transducer signal further depends on the quality of arrayed spots. Patterning surfaces and then spotting individual recognition units (multiplexing chemistry) is a way to produce small, information rich chips.

The adsorption of proteins on surfaces is a central concern in sensors and devices that contact biological fluids. Poly(ethylene glycol) (PEG) has been used in numerous biomedically relevant systems to control protein adsorption on surfaces[4-6]. For background passivation, different approaches have been proposed, according to the substrates employed[7]. Gold surfaces, in particular, are widely used for bioanalytic devices, especially those based on surface plasmon resonance (SPR) methods. Its conductivity, resistance to oxidation, and simplicity to produce thin and ultra flat films on inorganic substrates make this material particularly attractive.

A previous study of different patterning methods of PLL-*g*-PEG and their ensuing long term stability was performed by Lussi *et al.[8]*. The strength of the interaction between passivating molecule and the substrate determined the stability of the system. Therefore, it is thought that strong, multidentate interactions between a polymer and the underlying substrate may improve coating stability.

Thiol and thioether containing species are known to chemisorb onto gold, spontaneously forming self-assembled monolayers (SAMs) [9, 10]. The application of

SAM patterning [11] and SPR [12, 13] was previously reported in the literature; Kanda et al. demonstrated the fabrication of arrays with 64 spots on an ethylene-glycol-terminated SAM background[14]. Limitation of such systems lies in the relatively poor stability of chemisorbed alkanethiolates. Indeed, it has been shown that under ambient conditions substantial oxidation and subsequent loss of stability of alkanethiol SAMs takes place within days and the integrity of the adlayer is readily compromised[15, 16, 17]. As an alternative to thiol and thioether self-assembled monolayers, we have recently described chemisorption of a poly(propylene sulfide-*bl*-ethylene glycol) (PPS-PEG) triblock copolymer[18].This copolymer demonstrated high stability as assembled monolayer on gold, based on the availability of many chemisorption sites per adsorbate molecule as well as higher stability to oxidation of the sulfides in the chain thioether backbone (as compared to thiolates). In another study, a number of defined architectures of PPS-PEG were synthesized and adsorbed from methanol onto gold. Results obtained with human serum albumin (HSA) and serum (HS) indicated a close relationship between protein adsorption resistance and polymer architecture; symmetric triblocks of PPS-PEG with molecular weight of 5k/4k/5k and 2k/4k/2k were the most efficient in reducing protein resistance[19].

Commonly used protein patterning techniques include microcontact printing[1 , 20] [21]and photolithography[22, 23]. We modified the molecular assembly patterning by lift-off (MAPL) process documented by Falconnet[24], to accomplish our goals. MAPL is based on the use of the photoresist itself as the mask for localized surface functionalization. In the MAPL process, a photoresist pattern is transferred into a biochemical pattern by means of spontaneous adsorption and a subsequent photoresist lift-off. The process involves three basic steps: deposition and patterning of a photosensitive polymer (photoresist) on a substrate, assembly of a molecular system

and removal of the photoresist and excess material, resulting in a pattern of the assembled molecule on a bare substrate background. Pattern of both micro- and nanometer dimensions have been successfully prepared by this patterning method [24, 25]. The technique has been documented for niobia as the substrate with a pattern of a positive photoresist (Shipley S1818), where the pattern is transferred into functionalized poly(L-lysine)-graft-poly(ethylene glycol), PLL-g-PEG/PEG-X (X= biotin or cell adhesive peptide), and then backfilled with non-functionalized polymers from aqueous solutions.

SPR imaging is a label-free technique that can be employed to read microarrays[14, 26-30]. SPR is a common tool in bioanalytical chemistry - biomolecular interactions can be detected in real time with no labelling. SPR microscopy or SPR imaging provides the same advantages as SPR spectroscopy with the added feature of monitoring the adsorption with a spatial resolution down to a few microns on the sensing surface. The only modification of the spectroscopy system is replacement of the photodiode detector with a CCD camera. When adsorption of a molecule with a different refractive index than the solution takes place, the presence can be detected in a spatially resolved way by monitoring changes in reflected light intensity. These changes in reflected light intensity are proportional to the change in the refractive index near the surface at an angle near the SPR resonance angle, and can therefore be used for a semi-quanititive analysis of the protein resistance/adsorption of proteins on the surface.

MAPL patterning was adapted to the PPS-PEG block copolymer requirements and patterned substrates were characterized with ToF-SIMS and AFM. Patterned PPS-PEG gold substrates were then tested for protein resistance with SPR imaging.

Chemical backfilling of patterned surfaces was also explored and characterized with AFM.

2. Materials and Methods

Materials. All solvents were purchased from Fluka (Buchs, Switzerland) and used as received.

Symmetric triblock poly(propylene sulfide)-*block*-poly(ethylene glycol) (Fig.1) copolymers with a PPS backbone of 3.9 kDa molecular weight and two PEG end chains of 2kDa were synthesized and characterized as described elsewhere[19, 31]. The copolymers were added to methanol at a concentration of 1mg/ml and sonicated for a few seconds to mix.

47 nm gold layers with an intermediate layer of chromium (1.5 nm) were deposited on glass substrates (10x10mm or 20x20mm, Plano GmbH, Germany) using a Leybold direct current magnetron Z600 sputtering unit (PSI, Villigen, Switzerland). Prior to polymer adsorption, the surfaces were cleaned using a UV cleaner (Boekel Ind. Inc., PA, USA) for 30 min.

2.1. Molecular Assembly Patterning by Lift-off, (MAPL)

The standard MAPL patterning technique [24] was adapted for adsorption of PPS-PEG from aqueous to organic (methanol) solvent. Schematics of the production steps are shown in Fig 2.

Two positive photoresists were spun coated consecutively onto a 2x2 cm^2 gold substrates (4000 rpm for 40 s after having dried the substrate on a hot plate): LOR resist (Micro Chem, USA) with post baking at 150 °C for 5 min and S1818 (Shipley, USA) with post baking at 100 °C for 1 min. The LOR photoresist is desirable based on process chemical compatibility; we knew that the Shipley photoresist would grant

straight walled patterned structures (no undercut). Therefore the two photoresists were used in combination.

The photoresist was illuminated through a chromium mask (Photronics Switzerland) for 8 s with 500W power mercury lamp (exposure 80mJ/cm^2) and subsequently developed in 1:1 water/microposit 351 developer for 1 min with gentle shaking. S1818 was removed with 2 min ultrasonication in acetone, rinsed with the same solvent and dried with filtered nitrogen. Substrates were then rinsed in a water bath and finally dried with nitrogen.

The gold substrates, containing a patterned LOR were then dipped in a 1 mg/ml solution of PPS-PEG in methanol, rinsed with methanol after 45 min and dried with filtered nitrogen. The lift-off step was done in the following way: LOR was removed by soaking the substrate for 20 s in 1:2 N-methyl-pyrolidone (NMP for peptide synthesis, Fluka, Switzerland): ultrapure water and then for 10 s in only ultrapure water. Each sample was then placed vertically in a piranha-cleaned glass container with 10 ml NMP for 6 min. in an ultrasonic bath. After 30 s, half of the volume of NMP was replaced with fresh NMP. After 1 min the sample was transferred to a fresh piranha cleaned NMP containing glass. Finally, the sample was dipped in a 1:1 NMP: water glass container before washed in an ultrapure water bath for 5 min and dried with filtered nitrogen. This modified MAPL process leads to a pattern of PPS-PEG on gold. Bare gold regions then can be further modified with a second applicable chemistry.

2.2. Surface characterization techniques

Light microscopy.

The spatial fidelity of the photoresist was characterized by light microscopy (Zeiss Imager M1m, Switzerland) in epi-brightfield mode (reflection) with a 10x objective for the patterned photoresist on the gold substrates.

Variable angle spectrometric ellipsometry (VASE)

Ellipsometric data were measured with a variable angle spectrometric ellipsometer M-2000F (L.O.T. Oriel GmbH, Darmstadt, Germany).The measurement was conducted in the spectral range of 370-1000nm at three angles of incidence (65°, 70°, and 75°) under ambient conditions. VASE measurements were fitted with multilayer models using WVASE32 analysis software. The analysis of optical constants was based on a bulk gold layer, fitted for n and k on glass. After adsorption of PPS-PEG, the adlayer thickness was determined using a Cauchy model (A=1.45, B=0.01, C=0) [32]

Time-of-flight secondary ion mass spectroscopy (ToF-SIMS).

ToF-SIMS measurements were conducted on a PHI-TRIFT III instrument (Physical Electronics USA, Chanhassen, MN) equipped with a Gold (Au) liquid metal ion gun. The ion gun was operated at 22 KeV and the primary ion dose is below static SIMS limit. A bunched mode for high mass resolution was used first to acquire mass spectra. The typical mass resolution ~6000 was achieved in both positive and negative spectra.The positive spectra were calibrated using the secondary ion peaks CH3+, C2H3+, C3H5+, the negative spectra using CH-, OH-, C2H-. After careful calibration, chemical compositions of peaks of interest are identified. Prominent PEG-derived peaks in the positive and negative ion spectra were obtained based on the compilation of Wagner et al. Identified PEG or PPS fragments like C_2H_5O *and* C_3H_6S *were selected for further ToF-SIMS imaging analysis.* An un-bunched mode for high image resolution was then used to acquire ToF-SIMS images over an area of 400um x 400 um for 5 minutes.

Atomic force microscopy (AFM).

A Nanoscope IIIa-MultiMode AFM (Digital Instrument, USA) was used in contact mode with a Si_3N_4 tip and a 0.12 N/m spring constant. The force was maintained at the lowest possible value by adjusting the set point during imaging.

Surface plasmon resonance imaging (SPR-i)

The SPR system (Resonant Probes GmbH Goslar, Germany) used a monochromatic laser light source (633 nm) focussed onto a gold-coated glass slide (n=1.5230). Index matching between the 45° prism and the gold coated glass slide was achieved by using index matching oil (n_D25=1.7000 ± 0.0002, Cargille Labs, New Jersey, USA). The instrumental sensitivity measured for methanol is 0.003° with a baseline shift of 0.001°/min prior to PPS-PEG exposure. The experimental sensitivity is 0.03° if one looks at the methanol baseline rinsed with ethanol followed by a return to methanol.

2D information is obtained at a given angle by replacing the detector with a CCD camera[26]. Studies of the relationship between the reflectivity at a fixed angle showed that a range of imaging angles exists in which the reflectivity is linear for refractive index changes and thickness changes [14, 33]. Therefore, a semi-quantitative analysis of serum (Roche, Basel, Switzerland) adsorption on samples monitored in the image mode was performed. First, the CCD camera was focused onto the PPS-PEG pattern on the gold substrate in HEPES 2 solution. An angle scan between 53°-60° over the whole image as area of interest showed a minimum in light intensity proofing the presence of plasmons. The angle of incidence was fixed to a good light contrast at around 0.5° less than the minimum intensity. After a stable baseline was reached and the areas of interests were defined the surface was exposed to full human serum for 30 min followed by rinsing with HEPES 2 buffer.

3. Results and Discussion

The original MAPL technique, developed by Falconnet[24] could not be applied directly because the positive photoresist S1818 is soluble in methanol, the solvent of choice for the PPS-PEG adsorption. As an alternative to the S1818, LOR photoresist can be used. We covered the LOR with S1818 for the photolithographic step, removed the exposed S818 by 2 min ultrasonication in acetone, and then dipped the substrates with the patterned photoresist in the methanol solution. The patterning/ processing steps are represented schematically in Fig. 1.

The light microscopy images showed good quality of the photoresist pattern on the gold substrates (see fig.2). In order to quantify the adlayer thickness of the two spincoated photoresist layers, homogenous adlayers on gold substrates were tested for their thickness and quantified with ellipsometry (n=3). The LOR photoresist measured 453 ±4 nm thick and the S1818 measured 2052 ±2 nm thick (expected values,450 nm and 2000 nm, respectively). AFM images (50 μm x 50 μm) of the LOR resist on gold after complete removal of the S1818 denote a height distance step of 519 nm, which is consistent with the thickness measurements obtained with VASE (data not shown).

3.1. Pattern characterization by ToF-SIMS imaging and Atomic Force Microcopy imaging of PPS-PEG spots on gold substrates

The patterning method was characterized with two highly surface-sensitive analysis techniques: ToF-SIMS and AFM.

Fig. 3 shows ToF-SIMS images for the sum of all ion intensities in the positive ion spectra, the intensities of C_2H_5O, a typical fragment of PEG, the intensities of C_3H_6S, a typical fragment of PPS and the intensities of the gold (a-d). The figure shows ToF-SIMS images with a 60μm x 60 μm pattern with higher intensities for related PPS and

PEG fragments in the spots (3b and c) and higher intensities of gold (d) in the background. The gold ion intensity is much lower in the square pattern due to the presence of the PPS-PEG adlayer and the very shallow information depth (<1-2 nm) characteristic for the static ToF-SIMS technique, which is less than the PPS-PEG adlayer thickness.

AFM imaging in air was used as a complementary surface characterization technique employed to assess the quality of the spot definition. Using the AFM to characterize the pattern one would expect a contrast in height between the PPS-PEG adlayer on gold and the holes if the patterning of the PPS-PEG is successful. Figure 4, left side, shows a round spot (50 μm diameter) filled with chemisorbed PPS-PEG on a gold background after complete removal of the positive LOR photoresist. Even at higher magnification (see AFM insert) the pattern edges appear sharp and the spot as well as the bare Au background are homogenously smooth and uncontaminated. The layer thickness (4.0 nm) corresponds well with the thickness measured on homogenous PPS-PEG adlayers on gold with the same architecture (3.4 ± 0.4 nm, see ref.[19]), indicating that no polymer of the PPS-PEG spot was removed during the lift-off procedure and therefore the protein resistance should be maintained. Round spot sized of 20 μm diameter were reproduced with the same quality and potentially smaller features can be generated as well[25].

Finally, it is desirable that microarrays contain defined spots in a protein resistant background. Figure 4 (right side) represents the AFM image of patterned PPS-PEG by MAPL after backfill with PPS-PEG. Even if the spot front still can be detected in tapping mode the surface shows no longer a step height in the section analysis and the friction mode demonstrates the presence of a homogenous PPS-PEG layer and proves successful molecular backfill.

The modified MAPL approach produced well defined spots on the gold substrate. The step height measured with AFM and the chemical mapping with ToF-SIMS point to a complete and homogenous PPS-PEG adlayer inside the spots on a clean gold background.

3.2. Serum resistance of the MAPL approach characterized with SPR-*i*

Serum resistance test were performed with SPR-*i* for patterned substrates with PPS-PEG in the spots and bare gold as background. A large intensity change corresponds to less serum resistance. We averaged values over three different substrates, with five areas of interest in the PPS-PEG spots and five nearby. We measured intensity changes due to serum exposure of 6.6±4 mV in the spot and 100.5 ±14 mV on the gold background. Taking the gold background as reference, we measured a serum adsorption reduction of 93 % with SPR imaging. This finding is in good agreement with previously reported serum adsorption tests on homogenous PPS-PEG adlayers where a reduction up to 96 % was observed relative to bare gold[19]. This sound agreement in PPS-PEG layer thickness and serum resistance leads to the conclusion that a complete, reproducible, protein resistant PPS-PEG patterned monolayer is formed.

Further work will be devoted to the study of different patterning approaches, such as photochemical patterning. UV photopatterning is a straight forward method and has been applied to alkanethiolate SAMs by UV irradiation through a mask with micron-scale resolution[34]. This approach has been described for alkanethiols on gold[35], where sulfonate dominated the ToF-SIMS spectra in the area that was exposed to UV radiation. Oxidation of the thiol group results in a strong decrease of the binding energy in comparison to thiolates and oxidized SAMs, which do not coordinate

strongly with the gold and can be removed with rinsing. Since the chemisorption of PPS-PEG is also depending on Au-S interaction, we hypothesize that this approach could work for our system. A main concern with this technique is how to achieve sharp side walls and prevent a gradient of oxidized material from occurring around the edges of masked regions. An alternative strategy may be to photocatalytically pattern[36].

In context of applications of PPS-PEG adlayers in biomedical devices such as biosensors, the polymer adlayer stability is a critical issue in terms of shelf life. While PPS-PEG adlayers on gold surfaces turned out to be stable for at least 41 days, alkanethiols SAM were oxidized within two weeks of storage under ambient conditions[37]. PPS-PEG offers an increased stability for future gold biochip than alkanethiols.

4. Conclusions

We micropatterned gold substrates using PPS-PEG as background passsivation and the molecular assembly patterning by lift-off (MAPL) technique. Results show that the MAPL technique was successfully adapted for PPS-PEG adsorption requirements. Different geometric patterns were successfully transferred using photoresist to full and protein resistant PPS-PEG adlayers on a bare gold substrate backgrounds (20 μm circles to 60 μm squares). The MAPL approach is not limited to the micrometer scale, but may go down to the order of 100 nm as has been shown by Falconnet et al. [25]and should work for our system as well. The choice of micrometer scale pattern was made for the interest in biological applications such as the use of SPR-i in the biosensor area. The PPS-PEG/gold pattern may be backfilled with either oligo(EG)-

functionalized alkanethiol monolayers, or PPS-PEG polymers functionalized with a (bio)ligand grafted on the end of the PEG chains.

The combination of the MAPL technique, PPS-PEG and SPR-i has the potential to play an active role in the wide range of biosensing applications, in particular, protein analysis. The approach is label free and therefore has the potential to maintain the biological activity of the adsorbed proteins.

5. Acknowledgements

We thank Tobias Künzler and Brigitte Städler for the light microscopy images, Thomas Blättler and Christoph Huwiler for support in the photolithographic process. The FIRST team and especially Maria Leibinger are acknowledged for access to clean room conditions and support. Thanks to Didier Falconnet for assistance with the MAPL process. Whitney Hartung and Sara Morgenthaler aided the AFM measurements. We gratefully acknowledge funding from NIH R21 EB003991. This work was partially performed under the auspices of the U.S. Department of Energy by Lawrence Livermore National Laboratory under Contract W-7405-Eng-48 and in under Contract DE-AC52-07NA27344.

6. References

[1] A. Kumar, G. M. Whitesides, Applied Physics Letters 63 (1993) 2002-2004.
[2] D. C. Duffy, R. J. Jackman, K. M. Vaeth, K. F. Jensen, G. M. Whitesides, Advanced Materials 11 (1999) 546 - 552.
[3] J. Ziauddin, D. M. Sabatini, Nature 411 (2001) 107-110.

[4] A. Napoli, N. Tirelli, E. Wehrli, J. A. Hubbell, Langmuir 18 (2002) 8324-8329.
[5] P. Vermette, L. Meagher, Colloids and Surfaces B-Biointerfaces 28 (2003) 153-198.
[6] M. Morra, Journal of Biomaterials Science, Polymer Edition 11 (2000) 547 -- 569.
[7] C. M. Nelson, S. Raghavan, J. L. Tan, C. S. Chen, Langmuir 19 (2003) 1493-1499.
[8] J. W. Lussi, D. Falconnet, J. A. Hubbell, M. Textor, G. Csucs, Biomaterials 27 (2006) 2534-2541.
[9] R. G. Nuzzo, D. L. Allara, Journal of the American Chemical Society 105 (1983) 4481-4483.
[10] J. C. E. Love, L. A.; Kriebel, J. K.; Nuzzo, R. G.; Whitesides, G. M.;, Chem. Rev.; (Review) 105 (2005) 1103-1170.
[11] Z. Yang, W. Frey, T. Oliver, A. Chilkoti, Langmuir 16 (2000) 1751-1758.
[12] T. Wink, S. J. van Zuilen, A. Bult, W. P. van Bennekom, The Analyst 122 (1997) 43R - 50R.
[13] M. Mrksich, G. B. Sigal, G. M. Whitesides, Langmuir 11 (1995) 4383 - 4385.
[14] V. Kanda, J. K. Kariuki, D. J. Harrison, M. T. McDermott, Anal. Chem. 76 (2004) 7257-7262.
[15] M. Mrksich, L. E. Dike, J. Tien, D. E. Ingber, G. M. Whitesides, Experimental Cell Research 235 (1997) 305-313.
[16] M. J. Tarlov, J. G. Newman, Langmuir 8 (1992) 1398-1405.
[17] M. H. Schoenfisch, J. E. Pemberton, J. Am. Chem. Soc. 120 (1998) 4502-4513.
[18] J. P. Bearinger, S. Terrettaz, R. Michel, N. Tirelli, H. Vogel, M. Textor, J. A. Hubbell, Nature Materials 2 (2003) 259-264.
[19] L. M. Feller, S. Cerritelli, M. Textor, J. A. Hubbell, S. G. P. Tosatti, Macromolecules 38 (2005) 10503-10510.
[20] M. Mrksich, G. M. Whitesides, Trends in Biotechnology 13 (1995) 228-235.
[21] J. Lahiri, E. Ostuni, G. M. Whitesides, Langmuir 15 (1999) 2055-2060.
[22] C. H. Thomas, J. H. Collier, C. S. Sfeir, K. E. Healy, Proceedings of the National Academy of Sciences of the United States of America 99 (2002) 1972-1977.
[23] G. M. Whitesides, E. Ostuni, S. Takayama, X. Jiang, D. E. Ingber, Annual Review of Biomedical Engineering 3 (2001) 335-373.
[24] D. Falconnet, A. Koenig, F. Assi, M. Textor, Advanced Functional Materials 14 (2004) 749-756.
[25] D. Falconnet, D. Pasqui, S. Park, R. Eckert, H. Schift, J. Gobrecht, R. Barbucci, M. Textor, Nano Lett. 4 (2004) 1909-1914.
[26] J. S. Shumaker-Parry, C. T. Campbell, Anal. Chem. 76 (2004) 907-917.
[27] R. Rella, J. Spadavecchia, M. G. Manera, P. Siciliano, A. Santino, G. Mita, Biosensors and Bioelectronics 20 (2004) 1140-1148.
[28] B. P. Nelson, T. E. Grimsrud, M. R. Liles, R. M. Goodman, R. M. Corn, Anal. Chem. 73 (2001) 1-7.
[29] G. Steiner, V. Sablinskas, A. Hubner, C. Kuhne, R. Salzer, Journal of Molecular Structure 509 (1999) 265-273.
[30] B. Rothenhausler, W. Knoll, 332 (1988) 615-617.
[31] A. Napoli, N. Tirelli, G. Kilcher, J. A. Hubbell, Macromolecules 34 (2001) 8913-8917.
[32] E. Palik, Handbook of optical constants of solids, New York Academic, Orlando, 1985, p.
[33] T. Wilkop, Z. Wang, Q. Cheng, Langmuir 20 (2004) 11141-11148.

[34] M. J. Tarlov, D. R. F. Burgess, G. Gillen, J. Am. Chem. Soc 115 (1993) 5305-5306.
[35] J. Huang, H. J. C., J. Am. Chem. Soc. 115 (1993) 3342-3343.
[36] J. P. Bearinger, A. L. Hiddessen, K. J. J. Wu, A. T. Christian, L. C. Dugan, G. Stone, J. Camarero, A. K. Hinz, J. A. Hubbell, Biomolecular patterning via photocatalytic lithography, in: '(Ed.)'^'(Eds.)', NSTI Nanotech 2005, vol Anaheim, CA, 2005, p.^pp.
[37] J. Bearinger.

7.0 Figures/ Captions

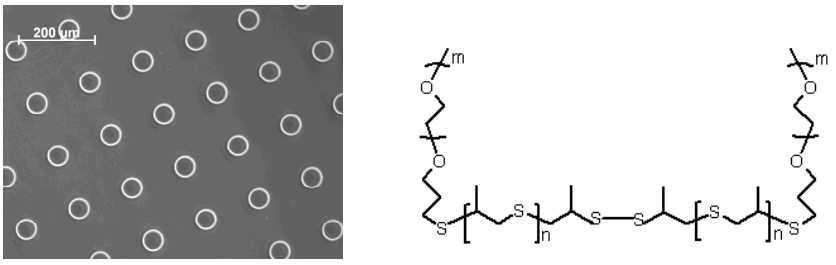

Fig. 1: Left: Light microscopy image of the mask showing a pattern of both photoresists on a gold substrate. Right: chemical structure of a symmetric PPS-PEG triblock copolymer (m=91 n=26).

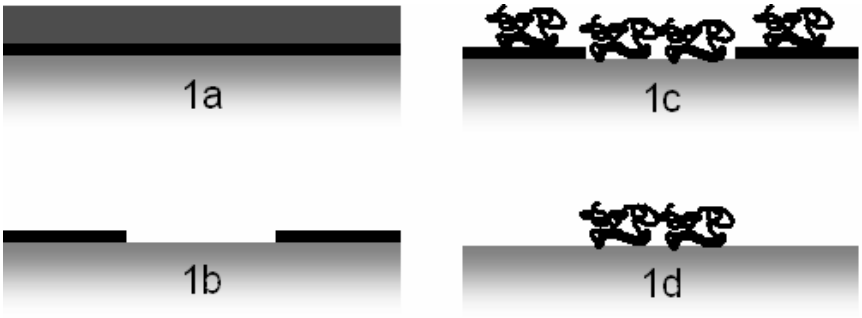

Fig.2: Schematic of the patterning processing steps employing the MAPL technique. Two positive photoresists (LOR and S1818) are spun coated onto gold substrates(1a). After illumination through a chromium mask, subsequent development and removal of the S1818 by ultrasonication in acetone for 2 min, a sharp pattern of photoresist (LOR) on the gold substrate is revealed (1b). PPS-PEG is adsorbed onto the patterned substrate with a dip-and-rinse process. During this step, the PPS-PEG chemisorbs on the unprotected areas of the gold substrate and physisorbs onto the LOR photoresist. (1c). The photoresist is removed by a lift-off resulting in a pattern of PPS-PEG on gold (1d).

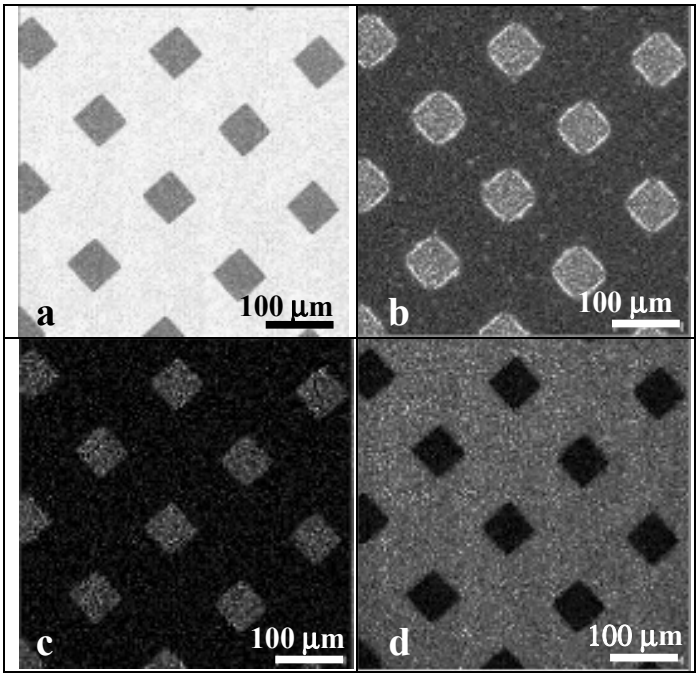

Fig. 3: ToF-SIMS mapping of surface chemistry for a MAPL surface of PPS-PEG adsorbed to 60 µm x 60 µm squares on a gold background. a.) Sum of positive ion intensities (total counts). b) Intensities representing C_2H_5O (m/q=45), a typical fragment of PEG. c) Intensities representing C_3H_6S (m/q=74), a typical fragment of PPS. d) Intensities representing gold (m/q=79).

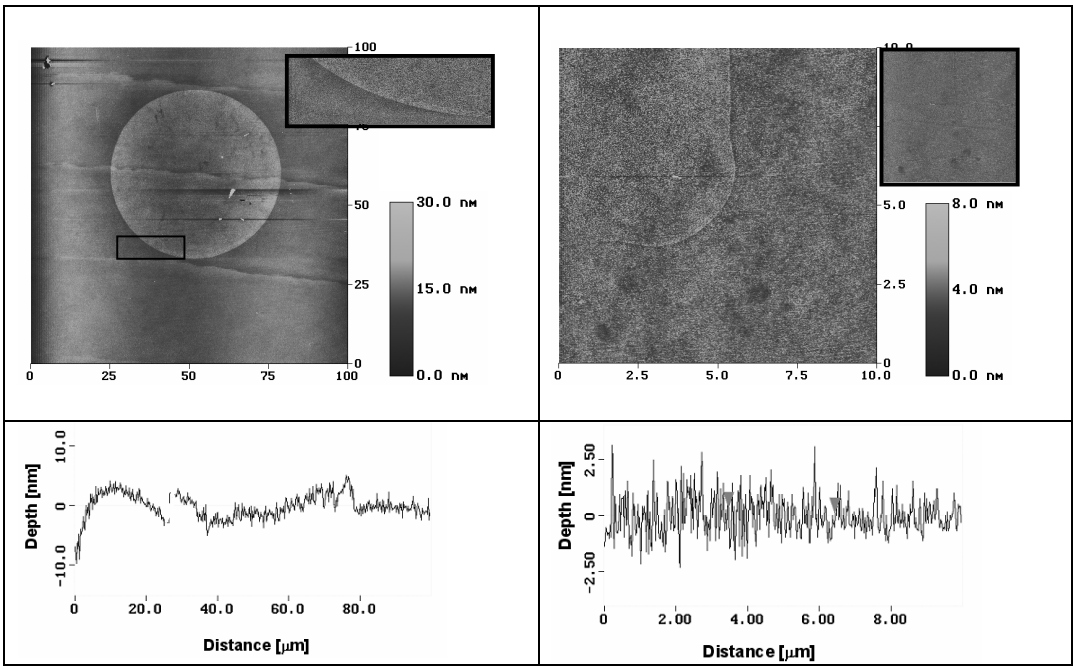

Fig. 4: (left) Tapping mode AFM showing the quality of a PPS-PEG spot on gold background (100μm). Inset shows spot definition. The depth profile shows step heights of the spot corresponding to the layer thickness of homogenous PPS-PEG. (right) Tapping mode AFM of PPS-PEG square spot produced via MAPL technique with subsequent backfill of the same polymer. Spot edge remains detectable although the average height inside and outside of spot is the same. Friction mode shows no difference inside versus outside of the spot (inset) suggesting no chemical contrast in either region.

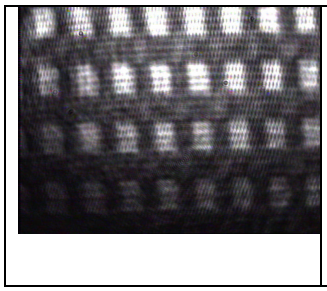

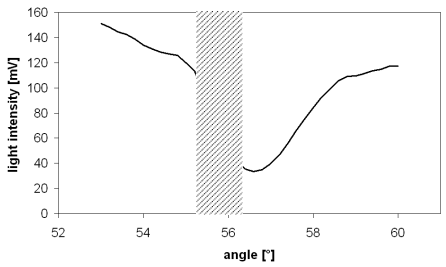

Intensity change **inside** the spots	6.6 ± 4mV
Intensity change **outside** the spots	100.5 ± 14mV
Reduction of serum adsorption	93%

Fig. 5: SPR-image of a 60 µm x 60 µm pattern in HEPES 2 buffer before serum exposure at an incoupling angle of 56.2° (left). Light intensity as a function of angle of incidence (middle, entire left image defined as area of interest and scanned for angles between 53 to 60°). The minimum of the reflected light shows the angle of the maximal excitation of the plasmons (56.2°). Five areas of interest were defined inside different spots containing a PPS-PEG adlayer and additional five areas nearby on the gold background were defined for testing the serum resistance of both surface chemistries at the same time. The table (right) summarizes the changes in light intensities before and after serum exposure collected at an angle of incidence where the change in light intensity is approximately proportional to the adsorption of mass on the area of interest (cross hatched region) (n=3).